HHS Public Access

Author manuscript

Cancer Lett. Author manuscript; available in PMC 2015 September 28.

Published in final edited form as:

Cancer Lett. 2014 September 28; 352(1): 97–101. doi:10.1016/j.canlet.2014.06.001.

Geometrical confinement of Gd(DOTA) molecules within mesoporous silicon nanoconstructs for MR imaging of cancer

Ayrat Gizzatov[1,2], **Cinzia Stigliano**[1], **Jeyerama S. Ananta**[1], **Richa Sethi**[2], **Rong Xu**[1], **Adem Guven**[2], **Maricela Ramirez**[1], **Haifa Shen**[1], **Anil Sood**[3], **Mauro Ferrari**[1,4], **Lon J. Wilson**[2], **Xuewu Liu**[1], and **Paolo Decuzzi**[1,*]

[1] Department of Translational Imaging and Department of Nanomedicine, The Methodist Hospital Research Institute, 6560 Fannin St, Houston, 77030, TX – USA.

[2] Department of Chemistry and the R.E. Smalley Institute for Nanoscale Science and Technology, Rice University, Houston, 77251-1892, TX – USA.

[3] Department of Gynecologic Oncology and Reproductive Medicine, The University of Texas MD Anderson Cancer Center, Houston, 77030 TX – USA.

[4] Department of Medicine, Weill Cornell Medical College, 1300 York Avenue, New York, 10065, NY – USA.

Abstract

Porous silicon has been used for the delivery of therapeutic and imaging agents in several biomedical applications. Here, mesoporous silicon nanoconstructs (SiMPs) with a discoidal shape and a sub-micrometer size (1,000 × 400 nm) have been conjugated with gadolinium-tetraazacyclododecane tetraacetic acid Gd(DOTA) molecules and proposed as contrast agents for Magnetic Resonance Imaging. The surface of the SiMPs with different porosities – small pore (SP: ~ 5 nm) and huge pore (HP: ~ 40 nm) – and of bulk, non-porous silica beads (1,000 nm in diameter) have been modified with covalently attached (3-aminopropyl)triethoxysilane (APTES) groups, conjugated with DOTA molecules, and reacted with an aqueous solution of $GdCl_3$. The resulting Gd(DOTA) molecules confined within the small pores of the Gd-SiMPs achieve longitudinal relaxivities r_1 of ~ 17 $(mM{\cdot}s)^{-1}$, which is 4 times greater than for free Gd(DOTA). This enhancement is ascribed to the confinement and stable chelation of Gd(DOTA) molecules within the SiMP mesoporous matrix. The resulting nanoconstructs possess no cytotoxicity and accumulate in ovarian tumors up to 2% of the injected dose per gram tissue, upon tail vein injection. All together this data suggests that Gd-SiMPs could be efficiently used for MR vascular imaging in cancer and other diseases.

* Corresponding author: pdecuzzi@houstonmethodist.org; +1 713 441 7316.

5. **Conflict of Interest Statement.** The authors declare no conflict of interest.

Keywords

Nanoconstructs; Magnetic Resonance Imaging; mesoporous silicon; relaxivity

1. Introduction

The use of nanoscale systems for the intravascular delivery of therapeutic and imaging agents has already had an impact in medicine.[1; 2; 3] Examples are given by the liposomal formulation of doxorubicin approved for the treatment of ovarian cancer, Kaposi sarcoma and multiple myeloma,[4] albumin-bound paclitaxel particles used for metastatic pancreatic cancer, non-small cell lung cancer and breast cancer,[5] and the albumin-bound gadolinium-tetraazacyclododecane tetraacetic acid (Gd-DOTA) complex approved for magnetic resonance angiography.[6] In addition, several other types of nanoscale systems are currently under development in clinical trials.[7] The nanoscale reformulation of therapeutic molecules and contrast agents has improved the circulation half-life, specific accumulation at the diseased site, with comparable or lower side effects to the original compound. The main advantage of nanoscale delivery systems is in their ability to be engineered and in their multifunctionality. Nanoparticles can be engineered with different sizes, shapes, and surface properties to enhance their in vivo performance [8; 9] and can simultaneously deliver multiple agents – both therapeutic and imaging agents – enabling the development of truly theranostic systems.[10; 11]

The main paradigm in the design of nanoparticles for cancer relies on the observation that the tumor blood vessels are discontinuous and present openings (fenestrations) as large as a few hundreds of microns.[12] Therefore, nanoparticles with a size of 100 – 200 nm could passively accumulate within the tumor tissue, mostly in a perivascular location, by crossing these endothelial fenestrations. However, in addition to the occurrence of vascular openings, tumors have more tortuous blood vessels and lack a well-developed lymphatic system, when compared to healthy tissue. This leads to an overall lower mean blood velocity (1 – 10 μm/sec) and high interstitial fluid pressure.[12; 13; 14] Taking advantage of these additional differences, we have engineered 1,000 × 400 nm discoidal mesoporous silicon particles (SiMPs) that will not cross the fenestrations but rather lodge within the tumor vasculature by adhering to the blood vessel walls. The SiMPs are comparable in size to platelets and, as such, tend to be pushed laterally by fast moving red blood cells[15], while the discoidal shape and sub-micrometer size of the SiMPs result in stable adhesion to the vessel walls in regions of low blood velocity.[9; 16; 17; 18] In healthy vessels, with more intense blood flow, the hydrodynamic dislodging forces tend to wash away the SiMPs preventing non-specific vascular adhesion. The authors have shown in two different tumor models, melanoma and orthotopic breast cancers, that such SiMPs accumulate up to 5% of the injected dose per gram tumor (% ID/g). [16; 19] Moreover, only SiMPs with a characteristic size larger than a few microns (> 2.0 μm) have been observed to massively accumulate within the microvasculature of the lungs.[20]

The mesoporous structure of the SiMPs has been efficiently loaded with several agents for cancer treatment and imaging. For instance, paclitaxel-containing polymer micelles and

nanoliposomes carrying siRNAs have been successfully encapsulated into SiMPs and used for the treatment of breast cancer.[21; 22; 23] Also, the mesoporous structure of the SiMPs has been loaded with gadolinium-(diethylene triamine pentaacetic acid) Gd(DTPA) molecules for MR imaging.[24; 25] In this case, the authors have shown that the geometrical confinement of Gd(DTPA) into the silicon mesopores enhances the MRI properties of the nanoconstructs leading to approximately a four-fold increase in longitudinal relaxivity r_1, as compared to clinically-available Gd-based contrast agents. Such an enhancement is associated with a decrease in water molecule mobility and rotational diffusivity of the Gd(DTPA) molecules. In this approach, however, the Gd(DTPA) molecules were non-specifically adsorbed on the walls of the silicon mesoporous matrix and, thus, were prone to be washed away upon systemic injection.

In this work, Gd^{3+}-ions have been covalently linked to the mesoporous silicon structure of the SiMPs by reacting Gd(DOTA) molecules with the amine groups on the (3-aminopropyl)triethoxysilane APTES-modified silicon surface both inside of pores and on the outer particle surface. Two different porous structures have been considered for the SiMPs: small pores (SiMP(SP)), where the average pore size is 5 nm and huge pores (SiMP(HP)), where the average pore size is larger than 40 nm. The amount of Gd^{3+}-ions per particle and the resulting MRI properties have been quantified for the two SIMP configurations and compared with those of conventional nonporous silica microspheres (SiMs) conjugated with Gd(DOTA) molecules only on the outer surface and not inside pores. Finally, the biological behavior of the Gd-SiMPs have been tested in vitro and in vivo upon systemic injection in mice bearing ovarian cancer.

2. Materials and Methods

2.1 Silicon particles

Discoidal porous silicon particles were fabricated by modification of our previously reported protocols.[24] The porous structures of the particles are tuned by adjusting electrochemical etching parameters while the particle dimensions are defined by photolithography. For this study, 1,000 nm (diameter) x 400 nm (thickness) porous silicon disks with two different pore sizes, specifically, 5-10 nm (small pore, SiMP(SP)), and ~ 40 nm (huge pore, SiMP(HP)), were fabricated. Briefly, starting with heavily doped p++ type (100) silicon wafers with resistivity of 0.005 ohm-cm (Silicon Quest, Inc, Santa Clara, CA) as the silicon source, 400 nm SP or HP layers was formed by anodic etching in hydrogen fluoride (HF) ethanolic solution. The 400 nm SP layer was etched by applying 2.3 mA/cm^2 current for 270 sec in a 3:7 HF (49%):ethanol solution, followed by applying 100 mA/cm^2 current for 8 sec to form the release layer. The etch condition for 400 HP layer was 7 mA/cm^2 current for 125 sec in a 1:3 HF (49%):ethanol solution. Following the formation of 400 nm SP, and HP layers, an 80 nm SiO_2 layer was deposited by Low Pressure Chemical Vapor Deposition at 400°C. Standard photolithography was used to pattern array of 1 μm circles on the SiO_2 layer using a contact aligner (K.Suss MA6 mask aligner) and NR9-500P photoresist (Futurrex Franklin, NJ, USA). The pattern was transferred into the porous silicon layer by reactive ion etching (RIE) in CF_4 plasma. The RIE system is a Plasmatherm 790, and the CF_4 flow conditions are: flow rate of 15 sccm; pressure of 100 mTorr; and RF power of 200

W. After stripping the capping SiO_2 layer in a ethanol solution (HF), the monodisperse particles were released from the substrate by sonication in isopropyl alcohol (IPA). The particles were treated with 35% H_2O_2 at 100°C for 2 hour to oxidize the surface, and then treated in 1N HNO_3 solution to increase the density of surface hydroxyl group. All the particles are fabricated in the Microelectronics Research Center at The University of Texas at Austin by a combination of standard photolithography and electrochemical etching. Volumetric particle size, size distribution and count were obtained using a Multisizer 4 Coulter® Particle Counter (Beckman Coulter, Fullerton, CA, USA).

2.2 Conjugation of the silicon particles with Gd(DOTA) molecules

The external surface of SiMPs was functionalized with Gd(DOTA) utilizing APTES chemistry. 1.0×10^9 SiMPs (HP or SP) were dispersed by brief sonication in 1 mL of v/v isopropyl alcohol/water (95/5) solution and 0.06 mL of (3-aminopropyl)trimethoxysilane (APTES) (97%, Alfa Aesar, MA, USA) were added. Reaction occurred in a shaker at 800 rpm and 50°C for 24 h. Then, SiMPs were centrifuged in water multiple times to remove unreacted APTES. The resulting APTES functionalized SiMPs were further reacted for 48h at room temperature with 60 mg DOTA (Sigma-Aldrich, USA) in the presence of 30 mg hydroxybenzotriazole (HOBt) and 60 mg of 1-ethyl-3-(3-dimethylaminopropyl)corbodiimide (EDC) as catalyst in 1 mL of 6 % MES buffer with the final pH adjusted to 6.1. At the end of the reaction, SiMPs where purified by centrifugation and redispersion in water multiple times. To coordinate Gd^{3+}-ions to the DOTA moiety on the surface of the SiMPs, the DOTA-conjugated SiMPs were exposed to 1 mL of 0.1 M aqueous $GdCl_3$ (Sigma-Aldrich, USA) solution and left to react under shaking conditions (400 rpm) for 24h at 24 °C. The resulting Gd-SiMPs nanoconstructs were purified multiple times via centrifugation from aqueous solution and used for the following characterizations. Non-porous silica microspheres 1.5 ± 0.08 μm (Polyscience, Inc., PA, USA) were functionalized following the same approach.

2.3 Physico-chemical characterization of the silicon particles

The Gd-SiMPs were characterized using transmission electron microscope (TEM) equipped with energy dispersive spectroscopy (EDS) to provide evidence of the present Gd^{3+}-ions on the surface of the Gd-SiMPs. For this, 10 μL of sample solution were dried on a TEM sample holder (Ted Pella, Inc., lacey formvar/carbon, 400 mesh Cu). The amount of coordinated Gd^{3+}-ions to the DOTA moieties of the Gd-SiMPs and Gd-SiMs nanoconstructs were assessed via inductively-coupled plasma optical emission spectrometry (ICP-OES) analysis. For this, the sample solution was first digested in 200 μL 99.99 % trace metals basis 1 M NaOH at 24 °C and then in 0.5 – 1 mL of 26% $HClO_3$ at 130 °C until dryness and reconstituted in 5 mL of 2 % HNO_3. The Gd-SiMPs were characterized with a scanning electron microscope (SEM) JEOL 6500F to assess structural changes before and after the end of the close to physiological condition challenge. For this, 20 μL of the sample solution was dried on the aluminum SEM specimen mount stubs (Electron Microscopy Sciences, PA, USA). The relaxivity properties of the Gd-SiMPs particles were characterized using a Bruker Minispec mq 60 benchtop relaxometer operating at 1.41 T and 37 °C with a 200 μL aqueous solution of sample contained in a 5 mm probe. MRI images were obtained for particles embedded in 1 % agarose gel using 3 T clinical MRI scanner (Philips Ingenia®).

2.4 Biological characterization of the silicon particles

To assess the stability of the Gd-SiMPs, under physiologically relevant conditions, 1X phosphate buffered saline (PBS) challenge was performed at pH = 7.4 under constant shaking (100 rpm) for up to 24 h at 37 °C. At each time point, particles were centrifuged and the concentration of the Gd^{3+}-ions was determined using ICP-OES in both the precipitate and the supernatant. To assess the in vitro cytotoxicity of the Gd-SiMPs, first HeLa cell lines were maintained at 37°C in water with low-glucose DMEM containing 10 % fetal calf serum, *l*-glutamine (2.9 mg/mL), streptomycin (1 mg/mL), penicillin (1000 units/mL), and saturated with air supplemented with 5 % CO_2. Cells were seeded in a 96-well cell plate and incubated for 24 h at 37 °C and 5 % CO_2. The cells were then incubated in fresh medium with different cell-to-nanoconstruct ratios. At the end of each time point, cytotoxicity was determined using an MTT assay.

2.5 Animal model and in vivo biodistribution analysis

In vivo biodistribution of the Gd-SiMPs were performed on a tumor-bearing mice model via tail vein injection of the 100 μl 5E8 Gd-SiMPs by count in 1X PBS solution. To evaluate the biodistribution of the Gd-SiMPs, mice were sacrificed 6 h post injection, organs were harvested, freeze-dried overnight, and digested in concentrated HNO_3 and 26 % $HClO_3$ with heat for Gd^{3+} analysis via the inductively-coupled plasma mass spectrometry (ICP-MS).

Female athymic nude mice were purchased from Charles River. The animals were maintained in cages with paper filter covers under controlled atmospheric conditions. Cages, covers, bedding, food, and water were changed and sterilized weekly. Animals were handled in a sterile manner in a laminar down-flow hood. All experimental procedures for animal studies were performed in accordance with regulation in the Houston Methodist Research Institute for the care and use of laboratory animals. HeyA8 cells (1×10^6) were injected intra-peritoneally into 6-week old female athymic nude mice. Tumor nodules in abdomen cavity were palpable 3 weeks post inoculation inoculation. These mice received a single dose of 1×10^9 Gd-SiMPs by tail vein injection. They were sacrificed 6 hours later, and major organs including liver, kidney, spleen and tumor nodules were collected.

3. Results and Discussions

Based on the favorable biodistribution behavior observed in previous studies [8; 19], here 1,000 × 400 nm discoidal mesoporous silicon particles (SiMPs) were considered with two different pore sizes, namely the small (SP) and huge pore (HP) SiMPs with an average pore diameter of ~ 5 nm and larger than 40 nm respectively and a commercially-available non-porous silica bead (SiO_2) with a diameter of 1,000 nm. As described in the Materials and Methods, the surface of these three nanoconstructs was first modified with (3-aminopropyl)trimethoxysilane (APTES) groups, then covalently conjugated with DOTA molecules, and eventually reacted with an aqueous solution of $GdCl_3$ to coordinate Gd^{3+}-ions with the DOTA moieties. The physico-chemical characterization of the SiMPs conjugates with Gd^{3+}-ions (Gd-SiMPs) is presented in **Figure.1**. The chemical structure of the SiMP and SiO_2 surface is depicted in **Figure.1a,** showing the Gd(DOTA) molecules directly bound to the APTES groups deposited over the nanoconstruct surfaces. In the TEM-

EDS spectrum illustrated in **Figure.1b**, characteristic peaks can be readily seen corresponding to Gd at 1 – 2 and 6 keV. The elemental spatial mapping for Si and Gd is presented in **Figure.1c,** demonstrating that the Gd^{3+}-ions are quite uniformly distributed over the mesoporous SiMP surface (Gd: red dots; Si: white dots).

A bench top relaxometer (Bruker Minispec, 1.41 T) was used to quantify the variation in longitudinal relaxation T_1, with respect to bulk water T_0, associated with the presence of the Gd^{3+}-ions on the surface of the silicon nanoconstructs. Then, ICP-OES was used to quantify the total amount of Gd^{3+}-ions per nanoconstruct. Thus, using the well-known relationship $r_1 = (1/T_1\text{-}1/T_0)/[Gd]$, the longitudinal relaxivity r_1 of the three nanoconstructs was determined for the Gd^{+3}-ion concentration [Gd]. The data are presented in **Figure.2a** for the three different nanoconstructs: SiMPs(HP) with huge pores (HP), SiMPs(SP) with small pores (SP) and the nonporous SiMs. It was observed that the Gd concentration per nanoconstruct increased going from the Gd-SiMPs(SP) (67±1.4 fM/particle), to Gd-SiMPs(HP) (121±4.2 fM/particle), and eventually to Gd-SiMs (171±60 fM/particle). On the contrary, the longitudinal relaxivity r_1 increased in the opposite direction being 8.09±2.1 $(mM{\cdot}s)^{-1}$ for the Gd-SiMs, 13.7±0.6 $(mM{\cdot}s)^{-1}$ for the Gd-SiMPs(HP), and reaching its maximum value of 16.8±1.9 $(mM{\cdot}s)^{-1}$ for the Gd-SiMPs(SP). Phantom images generated in a clinical 3T MRI scanner (**Figure.2b)** confirmed the significant higher relaxivity associated with the Gd-SiMPs than with the Gd-free SiMPs. In bulk solution, the Gd(DOTA) molecule presents a r_1 of ~ 4 $(mM{\cdot}s)^{-1}$ at 37° C and 1.41 T, whereas this relaxivity value grows up to ~ 17 $(mM{\cdot}s)^{-1}$ in a geometrically-confined configuration inside the SiMP pores.[26] This 4-fold enhancement in longitudinal relaxivity (r_1) is most likely associated with an increase of both the rotational correlation time (τ_R) for the Gd(DOTA) molecules (inner-sphere effect) and the diffusion correlation time (τ_D) for the water molecules (outer-sphere effect within the pores).[27] For the present Gd-SiO_2, the Gd(DOTA) molecules are not geometrically confined in any pore, thus the enhancement in relaxivity is mostly associated with an increase in τ_R leading to a r_1 of ~ 8 $(mM{\cdot}s)^{-1}$ (only 2-fold increase over free Gd(DOTA) molecules). For the Gd-SiMPs(HP), a 3-fold enhancement in relaxivity is observed with r_1 ~ 14 $(mM{\cdot}s)^{-1}$, which is most likely due to both an increase in τ_R and τ_D. This effect is even more evident with the Gd-SiMPs(SP), which are characterized by a smaller pore size (~ 5 nm), as compared to the Gd-SiMPs(HP), and provide a 4-fold increase in relaxivity (r_1 ~ 17 $(mM{\cdot}s)^{-1}$). [24; 25]

Given the significant enhancement in relaxivity with the Gd-SiMP(SP), these nanoconstructs were tested in a biologically relevant environment for their degradation over time, stability of the Gd^{3+}-ions conjugation to the silica surface, and cytotoxicity. For the degradation and stability tests, the Gd-SiMP(SP) were exposed to 1X phosphate buffered saline (PBS) solution, at pH = 7.4 and 37 °C, with constant shaking (100 rpm) for up to 24 h. **Figure.3a** shows scanning electron micrographs of Gd-SiMP(SP) at 0 and 24h post incubation. At 24h, the external rim of the Gd-SiMP(SP) is significantly remodeled, confirming that the mesoporous silicon particle degrades over time. This degradation process can be modulated by proper surface modification and the APTES layer deposited over the SiMP surface tend to decrease degradation rate and increase stability under physiological conditions.[28] Also, the progressive degradation is responsible for the release of any payload encapsulated within

the mesoporous structure, including the Gd(DOTA) molecules firmly conjugated to the surface undergoing slow erosion. As documented by the data presented in **Figure.3b**, almost 40% of the initial loading of Gd^{3+}-ions is released in the surrounding media after 24h of incubation. Importantly, no appreciable loss of Gd^{3+}-ions is observed within the first 6h post exposure to physiological conditions. SiMPs were also incubated with HeLa cell, as shown in **Figure.3c**. The darker dots in the bright field image represent Gd-SiMPs(SP) that have been uptaken by the HeLa cells at 24h post incubation. For the same cell line, a standard MTT assay was performed to assess potential cytotoxicity associated with the SiMPs and their Gd cargo. SiMPs were incubated with HeLa cells at different cell to particle ratios, ranging from 10 to 200, and at different time points, namely 24, 48, and 72 h (**Figure.3d**). No cell cytotoxicity was observed even for the lowest cell:nanoconstruct ratios (1:200) and for the longer incubation time (72h).

Finally, the in vivo biodistribution of the Gd-SiMPs were determined in mice bearing orthotopic ovarian tumors (**Figure.4**). Animals were injected via the tail vein with 1.0×10^9 Gd-SiMPs and sacrificed at 6h post injection. Previous studies have shown that SiMPs have a blood circulation half-life of the order of 1h [8], therefore the 6h time point is representative of the actual biodistribution of the particles, without incurring in any significant degradation and loss of Gd^{3+}-ions from the mesoporous matrix. The organ accumulation of Gd-SiMPs was quantified using ICP-MS and determining the concentration of Gd in the organs of the reticulo-endothelial system (RES) – liver, spleen, and kidney – and in the tumor (**Figure.4a**). As expected for all systemically injected particles, most of the Gd-SiMPs were observed to accumulate in the liver up to ~ 60% ID/g, followed by the spleen up to ~ 15% ID/g and kidneys up to ~ 5% ID/g. The accumulation in the neoplastic tissue was ~ 2% ID/g, which is comparable to several other systemically-injected nanoparticles. **Figure.4b** shows images of an ovarian tumor comprising several nodules, with a characteristic size ranging from a few millimiters to ~ 1 centimeter. In this image, especially the smaller nodules appear moderately perfused and this could justify the lower tumor accumulation observed for the Gd-SiMPs, as compared to previous data derived in more perfused breast cancer and melanoma models.

In conclusion, the high longitudinal relaxivity (r_1 ~17 $(m \cdot Ms)^{-1}$), the favorable tumor accumulation, and the stability under physiologically-relevant conditions of the present Gd-SiMPs represent a unique set of properties which can be capitalized upon development of the future effective and safe nanoconstructs for the Magnetic Resonance Imaging. Moreover, Gd-SiMPs are designed to lodge with the tumor vasculature and could provide information that are complementary to those offered by macromolecular imaging agents and small nanoparticles which, differently, are designed to directly target the tumor cells by crossing the fenestrated tumor vasculature.

Acknowledgements

This work was supported by the Cancer Prevention Research Institute of Texas through (grant CPRIT RP110262). We also thank the U.S. National Institutes of Health (grants U54CA143837 and U54CA151668) and the Welch Foundation (grant C-0627) for partial support.

References

1. Ferrari M. Cancer nanotechnology: opportunities and challenges. Nat Rev Cancer. 2005; 5:161–171. [PubMed: 15738981]
2. Schroeder A, Heller DA, Winslow MM, Dahlman JE, Pratt GW, Langer R, Jacks T, Anderson DG. Treating metastatic cancer with nanotechnology. Nat Rev Cancer. 2012; 12:39–50. [PubMed: 22193407]
3. Davis ME, Chen ZG, Shin DM. Nanoparticle therapeutics: an emerging treatment modality for cancer. Nat Rev Drug Discov. 2008; 7:771–782. [PubMed: 18758474]
4. Gabizon A, Catane R, Uziely B, Kaufman B, Safra T, Cohen R, Martin F, Huang A, Barenholz Y. Prolonged circulation time and enhanced accumulation in malignant exudates of doxorubicin encapsulated in polyethylene-glycol coated liposomes. Cancer Res. 1994; 54:987–992. [PubMed: 8313389]
5. Gradishar WJ, Tjulandin S, Davidson N, Shaw H, Desai N, Bhar P, Hawkins M, O'Shaughnessy J. Phase III trial of nanoparticle albumin-bound paclitaxel compared with polyethylated castor oil-based paclitaxel in women with breast cancer. J Clin Oncol. 2005; 23:7794–7803. [PubMed: 16172456]
6. Lauffer RB, Parmelee DJ, Dunham SU, Ouellet HS, Dolan RP, Witte S, McMurry TJ, Walovitch RC. MS-325: albumin-targeted contrast agent for MR angiography. Radiology. 1998; 207:529–538. [PubMed: 9577506]
7. Etheridge ML, Campbell SA, Erdman AG, Haynes CL, Wolf SM, McCullough J. The big picture on nanomedicine: the state of investigational and approved nanomedicine products. Nanomedicine. 2013; 9:1–14. [PubMed: 22684017]
8. van de Ven AL, Kim P, Haley O, Fakhoury JR, Adriani G, Schmulen J, Moloney P, Hussain F, Ferrari M, Liu X, Yun SH, Decuzzi P. Rapid tumoritropic accumulation of systemically injected plateloid particles and their biodistribution. J Control Release. 2012; 158:148–155. [PubMed: 22062689]
9. Decuzzi P, Pasqualini R, Arap W, Ferrari M. Intravascular delivery of particulate systems: does geometry really matter? Pharm Res. 2009; 26:235–243. [PubMed: 18712584]
10. Peer D, Karp JM, Hong S, Farokhzad OC, Margalit R, Langer R. Nanocarriers as an emerging platform for cancer therapy. Nat Nanotechnol. 2007; 2:751–760. [PubMed: 18654426]
11. Key J, Aryal S, Gentile F, Ananta JS, Zhong M, Landis MD, Decuzzi P. Engineering discoidal polymeric nanoconstructs with enhanced magneto-optical properties for tumor imaging. Biomaterials. 2013; 34:5402–5410. [PubMed: 23611451]
12. Jain RK, Stylianopoulos T. Delivering nanomedicine to solid tumors. Nat Rev Clin Oncol. 2010; 7:653–664. [PubMed: 20838415]
13. Hobbs SK, Monsky WL, Yuan F, Roberts WG, Griffith L, Torchilin VP, Jain RK. Regulation of transport pathways in tumor vessels: role of tumor type and microenvironment. Proc Natl Acad Sci U S A. 1998; 95:4607–4612. [PubMed: 9539785]
14. Chen X, Tohme M, Park R, Hou Y, Bading JR, Conti PS. Micro-PET imaging of alphavbeta3-integrin expression with 18F-labeled dimeric RGD peptide. Mol Imaging. 2004; 3:96–104. [PubMed: 15296674]
15. Lee TR, Choi M, Kopacz AM, Yun SH, Liu WK, Decuzzi P. On the near-wall accumulation of injectable particles in the microcirculation: smaller is not better. Sci Rep. 2013; 3:2079. [PubMed: 23801070]
16. van de Ven AL, Kim P, Haley O, Fakhoury JR, Adriani G, Schmulen J, Moloney P, Hussain F, Ferrari M, Liu X, Yun SH, Decuzzi P. Rapid tumoritropic accumulation of systemically injected plateloid particles and their biodistribution. J Control Release. 2011
17. Lee SY, Ferrari M, Decuzzi P. Shaping nano-/micro-particles for enhanced vascular interaction in laminar flows. Nanotechnology. 2009; 20:495101. [PubMed: 19904027]
18. Lee SY, Ferrari M, Decuzzi P. Design of bio-mimetic particles with enhanced vascular interaction. J Biomech. 2009; 42:1885–1890. [PubMed: 19523635]

19. Godin B, Chiappini C, Srinivasan S, Alexander JF, Yokoi K, Ferrari M, Decuzzi P, Liu X. Discoidal Porous Silicon Particles: Fabrication and Biodistribution in Breast Cancer Bearing Mice. Adv Funct Mater. 2012; 22:4225–4235. [PubMed: 23227000]

20. Decuzzi P, Godin B, Tanaka T, Lee SY, Chiappini C, Liu X, Ferrari M. Size and shape effects in the biodistribution of intravascularly injected particles. J Control Release. 2010; 141:320–327. [PubMed: 19874859]

21. Blanco E, Sangai T, Hsiao A, Ferrati S, Bai L, Liu X, Meric-Bernstam F, Ferrari M. Multistage delivery of chemotherapeutic nanoparticles for breast cancer treatment. Cancer Lett. 2013; 334:245–252. [PubMed: 22858582]

22. Shen H, Mittal V, Ferrari M, Chang J. Delivery of gene silencing agents for breast cancer therapy. Breast Cancer Res. 2013; 15:205. [PubMed: 23659575]

23. Shen H, Rodriguez-Aguayo C, Xu R, Gonzalez-Villasana V, Mai J, Huang Y, Zhang G, Guo X, Bai L, Qin G, Deng X, Li Q, Erm DR, Aslan B, Liu X, Sakamoto J, Chavez-Reyes A, Han HD, Sood AK, Ferrari M, Lopez-Berestein G. Enhancing chemotherapy response with sustained EphA2 silencing using multistage vector delivery. Clin Cancer Res. 2013; 19:1806–1815. [PubMed: 23386691]

24. Ananta JS, Godin B, Sethi R, Moriggi L, Liu X, Serda RE, Krishnamurthy R, Muthupillai R, Bolskar RD, Helm L, Ferrari M, Wilson LJ, Decuzzi P. Geometrical confinement of gadolinium-based contrast agents in nanoporous particles enhances T1 contrast. Nat Nanotechnol. 2010; 5:815–821. [PubMed: 20972435]

25. Sethi R, Ananta JS, Karmonik C, Zhong M, Fung SH, Liu X, Li K, Ferrari M, Wilson LJ, Decuzzi P. Enhanced MRI relaxivity of Gd(3+) -based contrast agents geometrically confined within porous nanoconstructs. Contrast Media Mol Imaging. 2012; 7:501–508. [PubMed: 22991316]

26. Laurent S, Elst LV, Muller RN. Comparative study of the physicochemical properties of six clinical low molecular weight gadolinium contrast agents. Contrast Media Mol Imaging. 2006; 1:128–137. [PubMed: 17193689]

27. Lauffer RB. Paramagnetic Metal-Complexes as Water Proton Relaxation Agents for Nmr Imaging - Theory and Design. Chemical Reviews. 1987; 87:901–927.

28. Godin B, Gu J, Serda RE, Bhavane R, Tasciotti E, Chiappini C, Liu X, Tanaka T, Decuzzi P, Ferrari M. Tailoring the degradation kinetics of mesoporous silicon structures through PEGylation. J Biomed Mater Res A. 2010; 94:1236–1243. [PubMed: 20694990]

Highlights

1. Gd(DOTA) is stably conjugated to mesoporous silicon nanoconstructs for MR imaging
2. Gd^{3+}-ions relaxivity is enhanced by 5 times as compared to clinical agents
3. Nanoconstructs accumulate up to 2% ID/g tissue in low perfused ovarian tumors

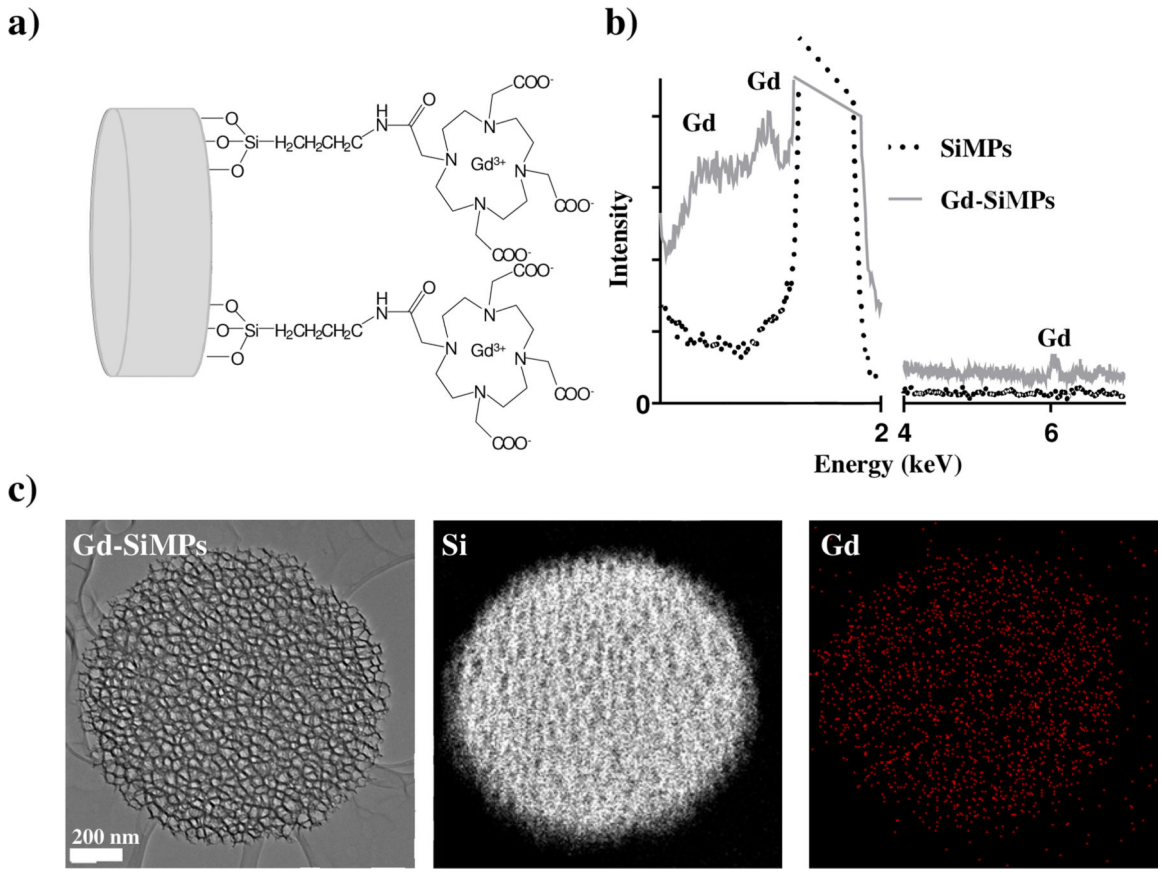

Figure 1. Physico-chemical analysis of the Gd-SiMPs

a) Schematic representation of the surface chemistry for the Gd-SiMPs. b) TEM-EDS spectra of Gd-SiMPs compared to Gd-free SiMPs. The Gd peaks appear at ~ 1 – 2 keV and 6 keV. c) TEM image and elemental mapping for Si and Gd of the Gd-SiMPs.

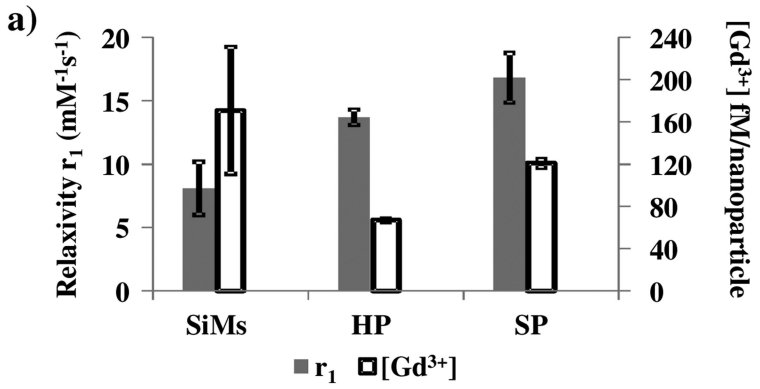

	Gd-SiMs	Gd-SiMPs(HP)	Gd-SiMPs(SP)
r_1 ($mM^{-1}s^{-1}$)	8.09 ± 2.1	13.7 ± 0.6	16.8 ± 1.9
[Gd^{3+}] fM/NP	171 ± 60	67 ± 1.4	121 ± 4.2

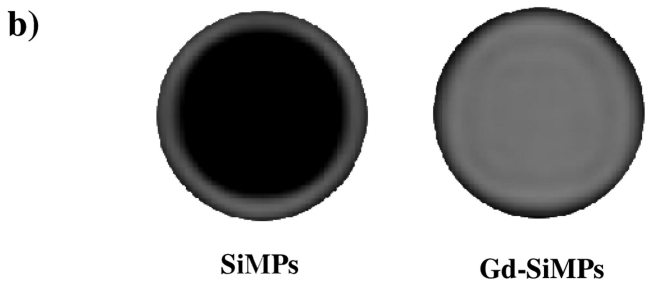

Figure 2. Characterizations of the Gd-SiMPs for magnetic resonance imaging

a,b) Longitudinal relaxivity (r_1) and concentration of Gd^{3+}-ions for the three different nanoconstructs, namely the Gd-SiMPs(HP) with huge pores; Gd-SiMPs(SP) with small pores; and the Gd-SiMs nonporous silica microspheres. c) T_1-weighted phantom images of SiMPs and Gd-SiMPs sample solutions obtained in a clinical 3T MRI scanner.

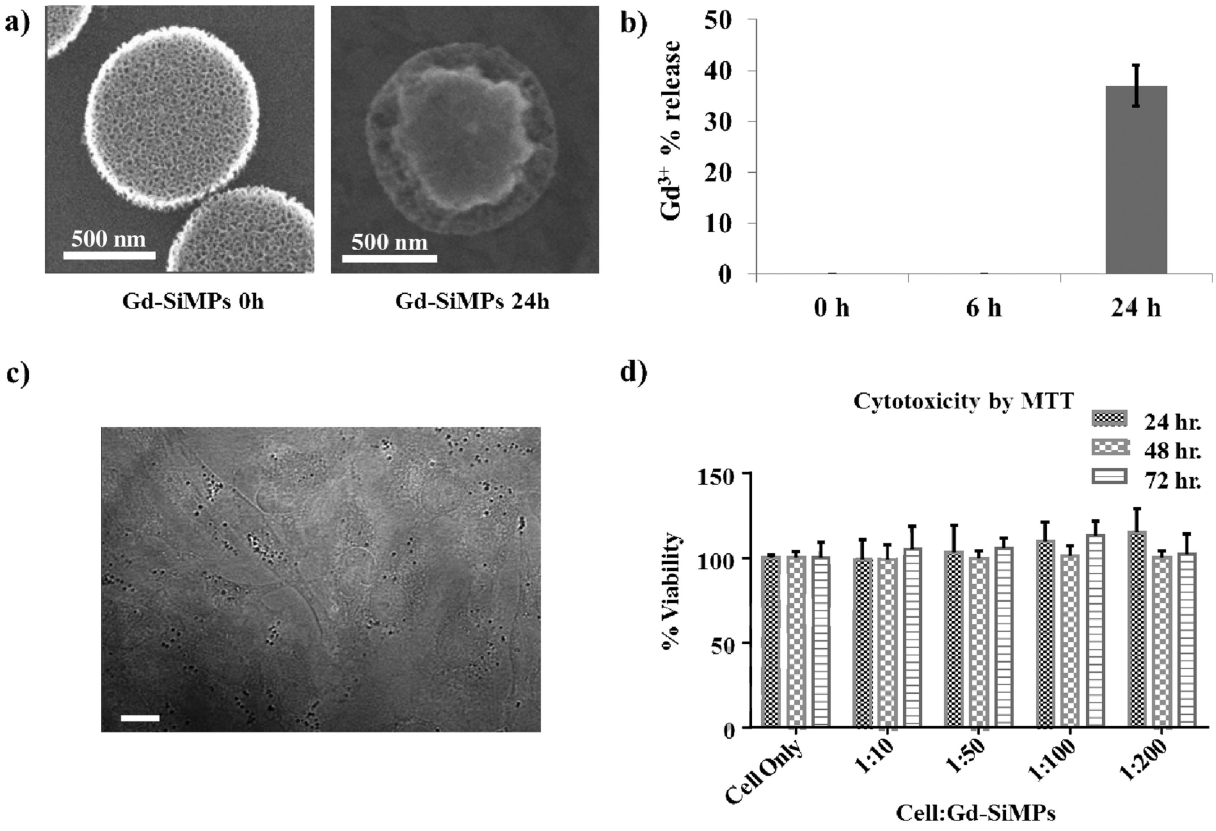

Figure 3. Biological characterization of the Gd-SiMPs

a) SEM images of the Gd-SiMPs before and after 24h incubation in PBS under constant shaking. b) Percentage release of Gd^{3+}-ions from the Gd-SiMP matrix upon incubation in PBS under constant shaking. c) Bright field microscopy images of HeLa cells and Gd-SiMPs (dark dots, scale bar = 10 μm). d) HeLa cell viability upon incubation with different concentrations of Gd-SiMPs, assessed via MTT assay at different time points.

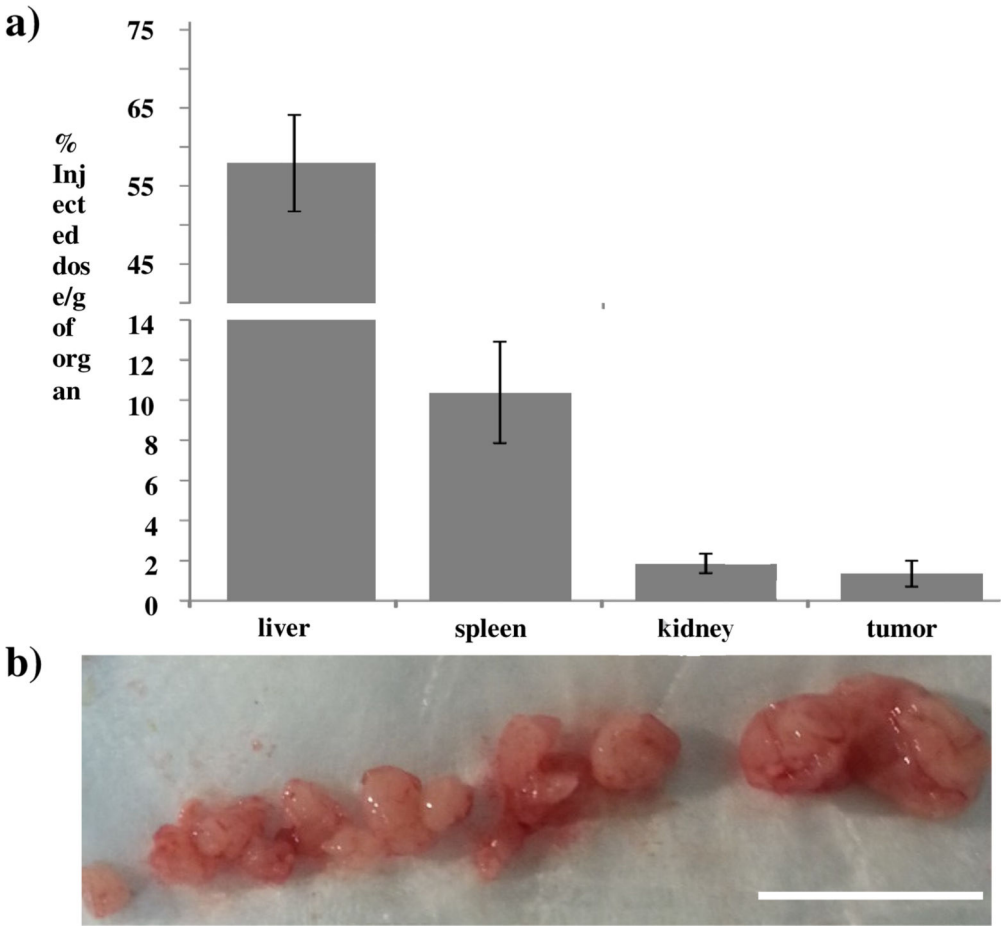

Figure 4. In vivo characterization of Gd-SiMPs

a) Biodisitrubtion of the Gd-SiMP nanoconstructs at 6h post injection in mice bearing ovarian cancer. The organ specific accumulation is expressed in percentage of the injected dose per gram organ (% injected dose/g of organ). (n = 5). b) Image of a nodular ovarian tumor with total weight of 1.54 g, showing multiple small nodules with moderately low perfusion (scale bar = 1 cm).